

# The polar clasps of a bank vole PrP(168–176) prion protofibril revisiting

Jiapu Zhang

*Centre of Informatics and Applied Optimisation, The Federation University Australia, Mount Helen Campus, Mount Helen, Ballarat, Victoria 3353, Australia;*

*\*Tel: +61-3-5327 6335; Email: j.zhang@federation.edu.au*

**Abstract:** On 2018-01-17 two electron crystallography structures (with PDB entries 6AXZ, 6BTK) on a prion protofibril of bank vole PrP(168-176) (a segment in the PrP  $\beta$ 2- $\alpha$ 2 loop) were released into the PDB Bank. The paper published by [Nat Struct Mol Biol 25(2):131-134 (2018)] reports some polar clasps for these two crystal structures, and "an intersheet hydrogen bond between Tyr169 and the backbone carbonyl of Asn171 on an opposing strand." - this hydrogen bond is not between the neighbouring Chain B and Chain A directly. In addition, by revisiting the polar clasps, we found another two hydrogen bonds (B.Asn171@H-A.Gln172@OE1, B.Tyr169@OH-A.Gln172@N) between the strand A of one sheet and the opposing strand B of the mating sheet. For the neighbouring two single  $\beta$ -sheets AB, the two new hydrogen bonds are completely different from the experimental one (an intersheet hydrogen bond between Tyr169 and the backbone carbonyl of Asn171 on an opposing strand) in [Nat Struct Mol Biol 25(2):131-134 (2018)].

**Key words:** PrP structured region · Fibril formation peptides · The ‘polar clasps’ · Mathematical formulas and optimizations · The hydrogen bonds

## 1 Introduction

Prion diseases were caused by the conformational change from normal cellular prion protein PrP<sup>C</sup> into diseased infectious prion PrP<sup>Sc</sup>. Numerous structures of PrP<sup>C</sup> are known and have been deposited into the Protein Data Bank (rcsb.org) (PDB). However, the atomic structure of the infectious, protease-resistant,  $\beta$ -sheet-rich and fibrillar mammalian PrP<sup>Sc</sup> remains unknown, being due to the unstable, noncrystalline and insoluble nature of the fibrils. Only during recent a decade the lab of Eisenberg DS at University of California Los Angeles and other labs are producing the atomic structures of some segments of PrP<sup>Sc</sup>. On 2018-01-17 two electron crystallography structures (with PDB entries 6AXZ, 6BTK) on a prion protofibril of bank vole PrP(168–176) (a segment in the PrP  $\beta$ 2- $\alpha$ 2 loop) were released into the PDB Bank. The structures belong to the ordinary Class 2 steric zipper with  $\beta$ -strands parallel and sheets pair front to back [1], but they have an outstanding hallmark: within a sheet there are very rich hydrogen bonds (HBs) - even constructing several ‘circles’ by polar residues Gln, Asn and Tyr of the two neighboring  $\beta$ -strands of a sheet; and between two neighboring  $\beta$ -sheets (if each is with one and only one  $\beta$ -strand) there are two additional HBs (B.Asn171@H-A.Gln172@OE1, B.Tyr169@OH-A.Gln172@N) too - besides the one of [2]. The authors named this character as ‘polar clasps’. This brief paper is revisiting the ‘polar clasps’ from the points of view in crystal mathematical formulas and mathematical optimization. Detailed HBs will be presented and illuminated for the ‘polar

clasps’.

First we introduce the definition of ‘polar clasps’ in [2]. ‘Polar clasp’ is a motif whose neighboring polar ladders in the PrP<sup>Sc</sup> are linked by HBs within a strand. Stacks of aromatic residues Phe175 and Tyr169 will shield these clasps at the core of PrP<sup>Sc</sup>.

In [3], the author showed us in Year 2016 a table listing all the PrP segments with cross- $\beta$  structures and each model is with its mathematical formulas and a color photo. Now we insert two elements ((21)–(22)) of bank vole (*Myodes glareolus*) PrP(168–176) of Year 2018 into the table and produce a new table, Tab. 1. We organize this paper as follows. Firstly, we present the approaches and tools that will be used in this paper and our major discovery about (molecular modelling) optimization skills will be given in the *Methods Section*. In the *Results and Discussion Section*, for models (21)–(22), the *first Subsection* will present mathematical formulas accompanied by graphs, then the *second Subsection* will revisit HBs of the ‘polar clasps’. Lastly, the *Summary Section* gives four concluding remarks.

Table 1: The cross- $\beta$  structures known in the PDB Bank of PrP segments:

PrP segment	Species	PDB ID	Class of the cross- $\beta$
(01) PrP(126–131)	human	4TUT	Class 7 <sup>[1, 4]</sup>
(02)	human-V129	4UBY	Class 8 <sup>[1, 4]</sup>
(03)	human-L129	4UBZ	Class 8 <sup>[1, 4]</sup>
(04) PrP(126–132)	human-L129	4W5L	Class 8 <sup>[1, 4]</sup>
(05)	human	4W5M	Class 8 <sup>[1, 4]</sup>
(06)	human-V129	4W5P	Class 8 <sup>[1, 4]</sup>
(07) PrP(127–132)	human	4WBU	Class 8 <sup>[1, 4]</sup>
(08)	human-V129	4WBV	Class 8 <sup>[1, 4]</sup>
(09)	human	3MD4	antiparallel (P 2 <sub>1</sub> 2 <sub>1</sub> 2 <sub>1</sub> )
(10)	human-V129	3MD5	parallel (P 1 2 <sub>1</sub> 1)
(11)	human	3NHC	Class 8 <sup>[1]</sup>
(12)	human-V129	3NHD	Class 8 <sup>[1]</sup>
(13) PrP(127–133)	human	4W5Y	Class 6 <sup>[1, 4]</sup>
(14)	human-V129	4W67	Class 6 <sup>[1, 4]</sup>
(15)	human-L129	4W71	Class 6 <sup>[1, 4]</sup>
(16) PrP(137–142)	mouse	3NVG	Class 1 <sup>[1]</sup>
(17) PrP(137–143)	mouse	3NVH	Class 1 <sup>[1]</sup>
(18) PrP(138–143)	Syrian hamster	3NVE	Class 6 <sup>[1]</sup>
(19)	human	3NVF	Class 1 <sup>[1]</sup>
(20) PrP(142–166)	sheep	1G04	$\beta$ -hairpin <sup>[5]</sup>
(21) PrP(168–176)	bank vole	6AXZ	Class 2 <sup>[2, 1]</sup>
(22)	bank vole	6BTK	Class 2 <sup>[2, 1]</sup>
(23) PrP(170–175)	human	2OL9	Class 2 <sup>[1]</sup>
(24)	elk	3FVA	Class 1 <sup>[1]</sup>
(25) PrP(177–182, 211–216)	human	4E1I	$\beta$ -prism I fold <sup>[6]</sup> (P 2 <sub>1</sub> 2 <sub>1</sub> 2 <sub>1</sub> )
(26)	human	4E1H	$\beta$ -prism I fold <sup>[6]</sup> (P 2 <sub>1</sub> 2 <sub>1</sub> 2 <sub>1</sub> )

## 2 Methods - The Molecular Modelling Approaches and Tools

The molecular modelling approaches used in the paper are the deep analyses for the files from the PDB library, optimization theory and the hybrid of optimization methods. The tools used are JSmol (<http://www.jmol.org>) - an open-source JavaScript computer software for molecular modelling chemical structures in 3-dimensions, VMD [7] (where the VMD is the most recent version VMD1.9.3Win32cuda downloaded from <http://www.ks.uiuc.edu/Research/vmd/>) - a molecular visualization program for displaying, animating, and analysing large biomolecular systems using 3-D graphics and built-in scripting, and the Swiss-PdbViewer 4.1.0 (<https://spdbv.vital-it.ch/>) [8, 9] - a free package for comparative protein modelling.

Optimization plays important roles in molecular modelling, and molecular simulations of molecular dynamics and/or quantum mechanics/molecular mechanics. Large-scale optimization computations have drawn considerable attention. The existing local/global optimization techniques effectively solve many problems when the number of variables is not very large and, as a rule, fail to solve many large-scale problems. The study of new algorithms which allow one to solve large-scale optimization problem is very important. One technique is to use hybrid of local/global and local/global search algorithms. This paper advocates the use of hybrid algorithmic approaches [10]. It is clearly possible that different optimization strategies would have made different results. In the second subsection of the Results and Discussion section we will use the hybrid of local search optimization methods Steepest Descent (SD) method + Conjugate Gradient (CG) method + Steepest Descent (SD) method when using Swiss-PdbViewer 4.1.0.

## 3 Results and discussion

### 3.1 Mathematical formulas and graphs

In this subsection, we will give the mathematical formulas for the fibrils of bank vole PrP(168–176) with PDB entries 6AXZ and 6BTK respectively, then we will illuminate their respective photos. The mathematical formulas can be gotten after reading the PDB files at websites:

<https://files.rcsb.org/view/6AXZ.pdb>, <https://files.rcsb.org/view/6BTK.pdb>, where the coordinates of the A Chain were given and we were told clearly “APPLY THE FOLLOWING TO CHAINS: A” to get other Chains. Their photos can be gotten from the websites <https://www.rcsb.org/3d-view/6AXZ/1>, <https://www.rcsb.org/3d-view/6BTK/1> respectively by selecting the viewer JSmol (JavaScript).

### 3.1.1 PDB entry 6AXZ – bank vole PrP(168–176)

Model (21): In Fig. 1 we see that B chain (i.e.  $\beta$ -sheet 2) of 6AXZ.pdb can be obtained from A chain (i.e.  $\beta$ -sheet 1) by

$$B = A + \begin{pmatrix} -2.18510 \\ 10.10648 \\ 0 \end{pmatrix}, \quad (1)$$

and other chains can be got by

$$C(D) = A(B) + \begin{pmatrix} 4.94 \\ 0 \\ 0 \end{pmatrix}, \quad (2)$$

$$E(F) = A(B) + \begin{pmatrix} 2 * 4.94 \\ 0 \\ 0 \end{pmatrix}, \quad (3)$$

$$G(H) = A(B) + \begin{pmatrix} 3 * 4.94 \\ 0 \\ 0 \end{pmatrix}, \quad (4)$$

$$I(J) = A(B) + \begin{pmatrix} 4 * 4.94 \\ 0 \\ 0 \end{pmatrix}. \quad (5)$$

### 3.1.2 PDB entry 6BTK – bank vole PrP(168–176)

Model (22): In Fig. 2 we see that B chain (i.e.  $\beta$ -sheet 2) of 6BTK.pdb can be obtained from A chain (i.e.  $\beta$ -sheet 1) by

$$B = A + \begin{pmatrix} -2.04266 \\ 9.89843 \\ 0 \end{pmatrix}, \quad (6)$$

and other chains can be got by

$$C(D) = A(B) + \begin{pmatrix} 4.874 \\ 0 \\ 0 \end{pmatrix}, \quad (7)$$

$$E(F) = A(B) + \begin{pmatrix} 2 * 4.874 \\ 0 \\ 0 \end{pmatrix}, \quad (8)$$

$$G(H) = A(B) + \begin{pmatrix} 3 * 4.874 \\ 0 \\ 0 \end{pmatrix}, \quad (9)$$

$$I(J) = A(B) + \begin{pmatrix} 4 * 4.874 \\ 0 \\ 0 \end{pmatrix}. \quad (10)$$

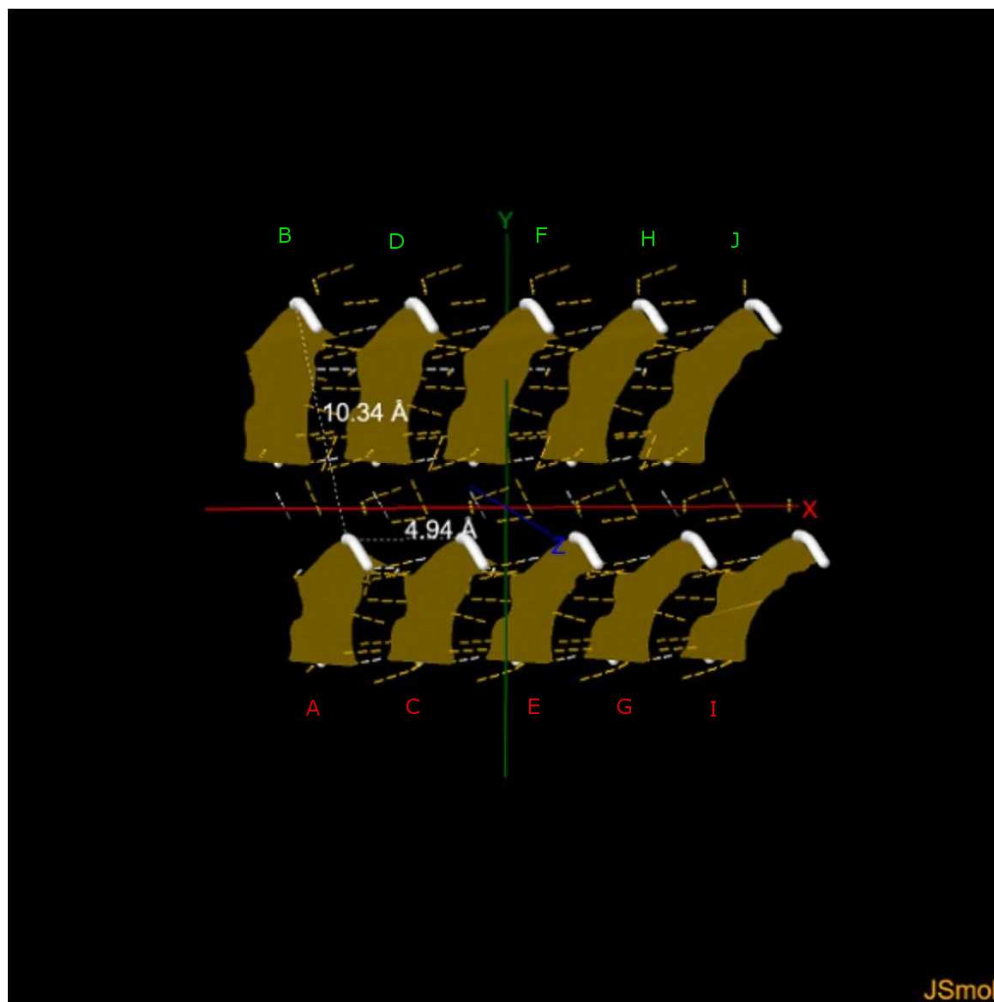


Figure 1: Protein fibril structure of QYNNQNNFV segment 168–176 from bank vole prion (PDB entry 6AXZ). The dashed lines denote the HBs. A, B, ..., I, J denote the 10 chains of the fibril.

### 3.2 Revisiting the HBs

We used the above mathematical formulas and the Figs. 1-2 to get (I) *AC-Chains* and (II) *AB-Chains* for 6AXZ.pdb and 6BTK.pdb respectively, and (III) *ABCD-Chains* for 6AXZ.pdb. We used VMD to visualize the HBs of (I)–(III) for each pdb but we cannot find HBs yet (where the HB parameters are the default ones of VMD: Donor-Acceptor Distance Cutoff 3.0 Å, Angle cutoff 20 degrees). Thus we used Swiss-PdbViewer 4.1.0 (the file SPDBV\_4.10\_PC.zip downloaded from <https://spdbv.vital-it.ch/>) to optimize (I)–(III) (Tab. 2), where we found the hydrogen atoms were added after the optimization by the Swiss-PdbViewer.

The Swiss-PdbViewer is the most recent version Swiss-PdbViewer 4.1.0 and we set the Energy Minimization Preferences as follows: 100 Steps of Steepest Descent (SD) method, then 100 Steps of Conjugate Gradient (CG) method, and at last 50 Steps of

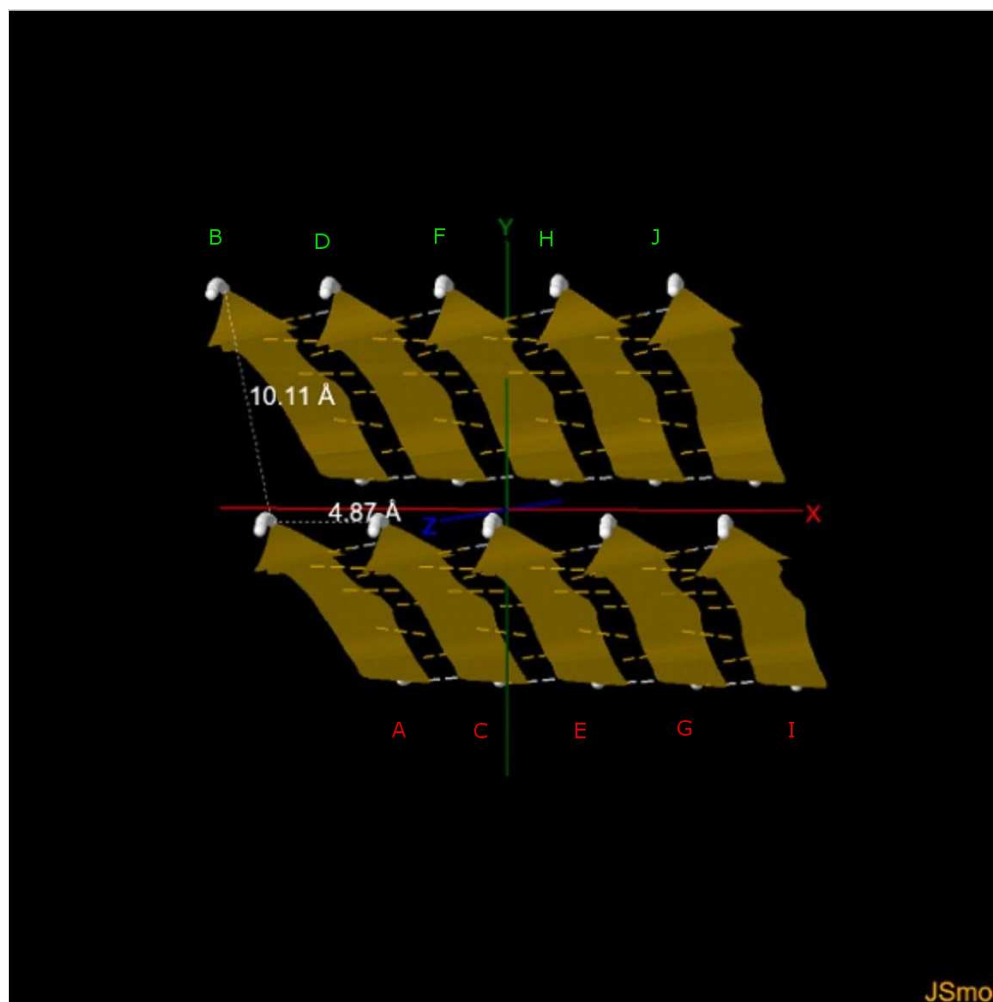


Figure 2: Protein fibril structure of QYNNQNNFV segment 168–176 from bank vole prion (PDB entry 6BTK). The dashed lines denote the HBs. A, B, ..., I, J denote the 10 chains of the fibril.

SD method to slightly optimize the model - i.e. here we used the hybrids of SD-CG-SD optimization methods. The optimization considered the Bonds, Angles, Torsions, Improper, Non-bonded, Electrostatic, and we selected the Cutoff as  $12.000 \text{ \AA}$ . The stopping criteria when delta E between two steps is below  $0.050 \text{ KJ/mol}$  and when Force acting on any atom is below  $10.000$  are selected. The computations were done in vacuo with the GROMOS96 43B parameters set, without reaction field, and the energy computations were done with the GROMOS96 implementation of Swiss-PdbViewer 4.1.0.

After the optimization, we got the HBs network for (I)–(III) respectively (Tabs. 3-5), where the HB detection threshold parameters are the default ones of Swiss-PdbViewer 4.1.0: when Hydrogens are present, Min cutoff distance  $1.200 \text{ \AA}$ , Max cutoff distance  $2.760 + 0.050 \text{ \AA}$ , Min Cutoff Angle  $120.000$  degrees; and when Hydrogens are not present, Min cutoff distance  $2.195 \text{ \AA}$ , Max cutoff distance  $3.300 + 0.050 \text{ \AA}$ , Min

Table 2: The energy decreases during the optimization:

PrP segment	Species	PDB ID	Chains	Energy (KJ/mol) decreases
(21) PrP(168–176)	bank vole	6AXZ	AC	-2250.996 → -2264.804 → -2268.384
			ACE	-3617.681 → -3635.713 → -3646.515
			ABCD	-4706.212 → -4715.012 → -4726.107
			AB	-1885.567 → -1901.603 → -1904.400
(22)	bank vole	6BTK	AC	-2268.958 → -2269.830 → -2274.719
			ACE	-3664.371 → -3674.300 → -3678.038
			AB	-1916.021 → -1919.213 → -1922.448

Cutoff Angle 90.000 degrees.

(I) *AC-Chains*. There are 20 HBs for the optimized AC Chains of 6AXZ and 6BTK respectively (Tab. 3 and Fig. 3). Here we found 14 interchain HBs, including the 6 interchain HBs in Fig. 2 of [2] labeled by blue arrows.

Table 3: The 20 HBs between the optimized AC Chains or within its each Chain for each pdb model:

between C–A Chains	in A Chain	in C Chain
Val176@H–Phe175@O	Asn174@OD1–Gln172@H	Asn174@OD1–Gln172@H
Asn174@O–Phe175@H	ASN171@OD1–Asn173@H	Asn171@OD1–Asn173@H
Asn174@H–Asn173@O	Asn170@H–Gln168@OE1	Asn170@H–Gln168@OE1
Asn174@H–Asn174@OD1		
Asn173@OD1–Asn173@H		
Gln172@H–Asn171@O		
Gln172@OE1–Gln172@H		
Gln172@O–Asn173@H		
Asn171@OD1–Asn171@H		
Asn170@O–Asn171@H		
Asn170@H–Asn170@OD1		
Asn170@H–Tyr169@O		
Gln168@O–Tyr169@H		
Gln168@OE1–Gln168@H		

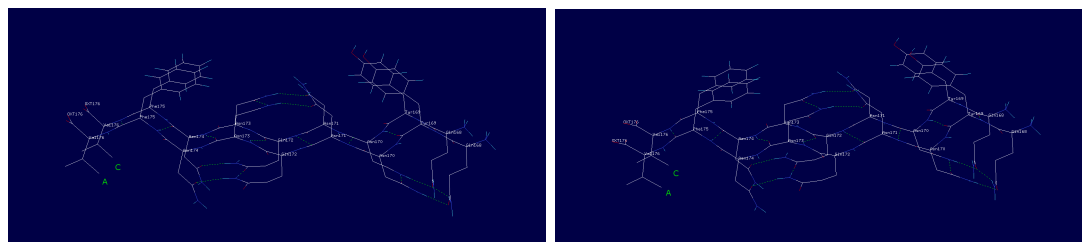


Figure 3: The optimized AC Chains in the fibril structures of QYNNQNNFV segment 168–176 from bank vole prion (left: 6AXZ, right: 6BTK). The dashed lines denote the HBs. The photos were produced by Swiss-PdbViewer 4.1.0. The green coloured A and C denote the A Chain and C Chain respectively.

(II) *AB-Chains*. There are 7 HBs for the optimized AB Chains of 6AXZ and

6BTK respectively (Tab. 4 and Fig. 4). Here the single intersheet HB Asn171@H–Gln172@OE1 is different from the one in Fig. 2 of [2] labeled by a red arrow (a note: if we set the *Max distance* 3.4 Å when *Hydrogens* are not present, we can find a HB *B.Tyr169@OH–A.Gln172@N* with distance 3.44 Å (Fig. 5) where the coordinate of *B.Tyr169@OH* is (-3.491, 1.826, 6.481), the coordinate of *A.Gln172@N* is (-1.581, -0.424, 8.254), and *B Chain* is got from *A Chain* by mathematical formula (6). We should notice here the AB Chains are not optimized yet). The intrachain three HBs labeled by orange arrows in Fig. 2 of [2] are found here (see Tab. 4 and Fig. 4).

Table 4: The 7 HBs between the optimized AB Chains or within its each Chain for each pdb model:

between B–A Chains	in A Chain	in B Chain
Asn171@H–Gln172@OE1	Asn174@OD1–Gln172@H Asn173@H–Asn171@OD1 Asn170@H–Gln168@OE1	Asn174@OD1–Gln172@H Asn173@H–Asn171@OD1 Asn170@H–Gln168@OE1

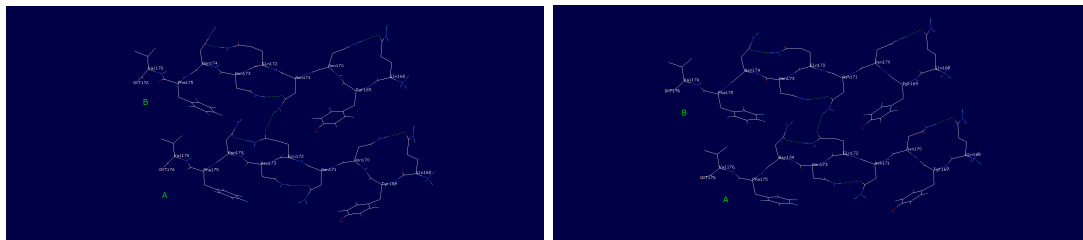


Figure 4: The optimized AB Chains in the fibril structures of QYNNQNNFV segment 168–176 from bank vole prion (left: 6AXZ, right: 6BTK). The dashed lines denote the HBs. The photos were produced by Swiss-PdbViewer 4.1.0. The green coloured A and B denote the A Chain and B Chain respectively.

The AB sheets stack in a parallel face-to-back configuration, the convex face of sheet A nestles against the concave back of its neighboring sheet B, with a high degree of surface complementarity (Fig. 4). Seeing Fig. 6, in AB Chains, the most colored in pink are the polar residues Gln168–Asn174, another color of residues are the hydrophobic residues Phe175 and Val176.

(III) *ABCD-Chains*. In ABCD Chains, 28.9% of the atoms are hydrogen. There are a lot of HBs for the optimized ABCD Chains of 6AXZ model (see Fig. 7, and the supplementary Tab. 2 of [2] where B is the C in here and C is the B here), including the Asn171@H–Gln172@OE1 in Tab. 4 linking B and A Chains, the HBs Asn171@O–Tyr169@H and Asn174@H–Asn173@OD1 linking A and D Chains, and Gln172@OE1–Asn171@H linking C and D Chains (Tab. 5 and Fig. 7).

By Figs. 7-8 and Tab. 5, we can confirm the “intersheet hydrogen bond between Tyr169 (of D Chain) and the backbone carbonyl of Asn171 (of A Chain) on an opposing



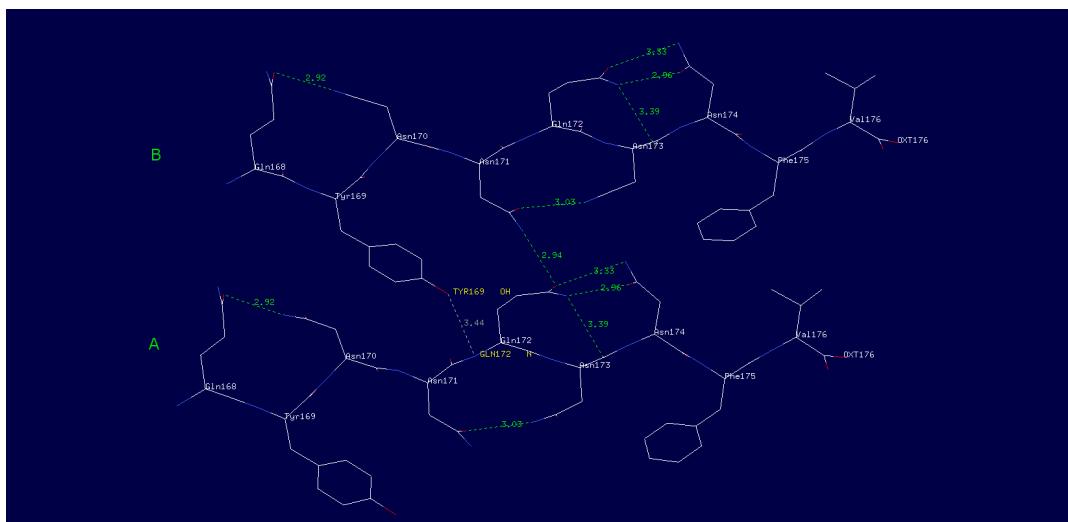


Figure 5: The HB B.Tyr169@OH–A.Gln172@N between AB Chains (not optimized yet, directly got by mathematical formula (6)) in the fibril structures of QYNNQNNFV segment 168–176 from bank vole prion (6BTK.pdb). The dashed lines denote the HBs. The photo was produced by Swiss-PdbViewer 4.1.0.

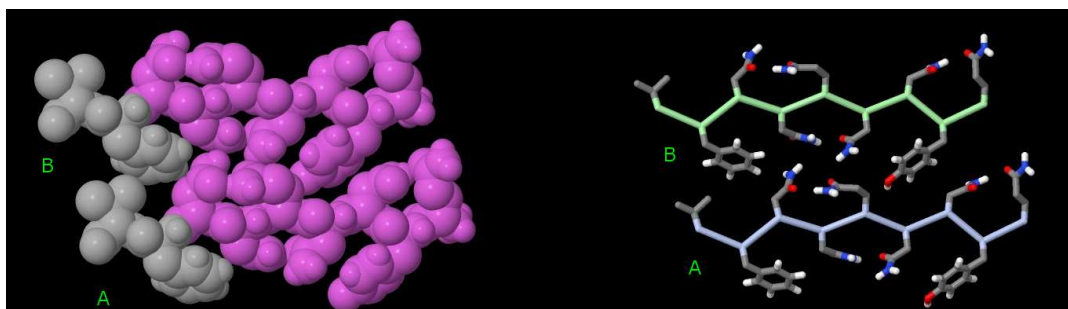


Figure 6: The distributions of residues of AB Chains in the fibril structures of QYNNQNNFV segment 168–176 from bank vole prion (PDB entry 6AXZ). Pink: polar residues Gln168–Asn174, gray: hydrophobic residues Phe175–Val176.

Table 5: The 4 special HBs between the optimized ABCD Chains for the 6AXZ.pdb model:

The pair of Chains	HBs
BA	Asn171@H–Gln172@OE1
AD	Asn171@O–Tyr169@H, Asn174@H–Asn173@OD1
CD	Gln172@OE1–Asn171@H

strand” of [2], bearing in mind that

$$D = A + \begin{pmatrix} -2.18510 + 4.94 \\ 10.10648 \\ 0 \end{pmatrix}. \quad (11)$$

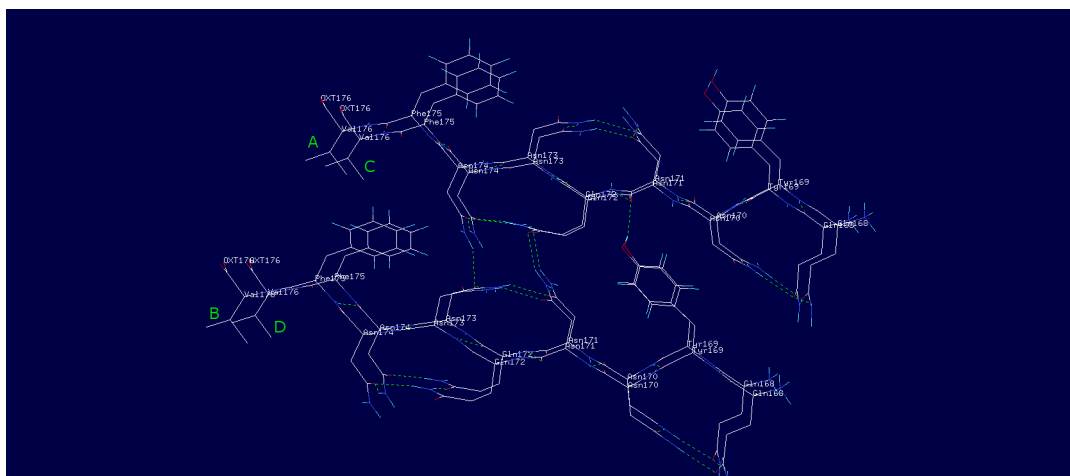


Figure 7: The optimized ABCD Chains in the fibril structures of QYNNQNNFV segment 168–176 from bank vole prion (PDB entry 6AXZ). The dashed lines denote the HBs. The photos were produced by Swiss-PdbViewer 4.1.0.

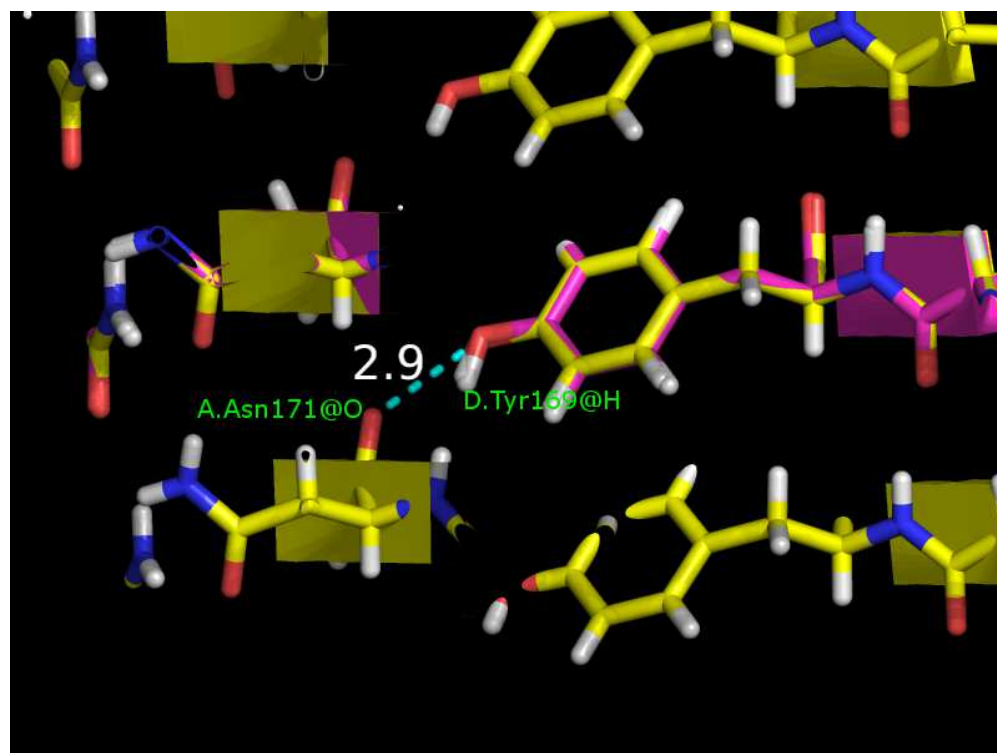


Figure 8: The HB A.Asn171@O–D.Tyr169@H between the optimized AD Chains in the fibril structures of QYNNQNNFV segment 168–176 from bank vole prion (6AXZ.pdb). The dashed lines denote the HB. The photo was offered by Rodriguez JA (University of California Los Angeles).

At the end of this subsection, we revisit the HBs of the optimized ACE Chains. We illuminate them in Fig. 9, where there are some ‘polar clasps’ (as shown in the supplementary Fig. 7 of [2]).

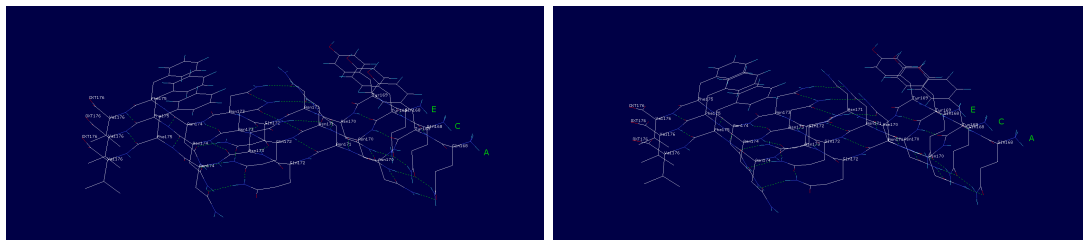


Figure 9: The optimized ACE Chains in the fibril structures of QYNNQNNFV segment 168–176 from bank vole prion (left: 6AXZ, right: 6BTK). The dashed lines denote the HBs. The photos were produced by Swiss-PdbViewer 4.1.0. The green coloured A, C, E denote the A Chain, C Chain and E Chain respectively.

## 4 Summary

This short paper revisited the ‘polar clasps’ and presented detailed HBs of the ‘polar clasps’. We found out more HBs for the neighboring two  $\beta$ -strands, for the block of two  $\beta$ -sheets - each sheet being with two  $\beta$ -strands, and the most important, for the neighboring two single  $\beta$ -sheets AB, two new HBs B.Asn171@H–A.Gln172@OE1, B.Tyr169@OH–A.Gln172@N were found out, which is completely different from the experimental one (an intersheet HB between Tyr169 and the backbone carbonyl of Asn171 on an opposing strand) in [2].

The structures of some segments of PrP<sup>Sc</sup> have been determined, including the most recent bank vole PrP<sup>Sc</sup>(168–176) one of [2]. In Fig. 16.3 of [11], we have predicted that some segments PrP(126–133), PrP(137–143), PrP(168–176), PrP(170–175), PrP(177–182), PrP(211–216) should have the amyloid fibril forming property.

This brief paper also showed us the importance of optimization. Before optimization, we could not find out any HBs (where the distance and angle cutoffs are the default values of VMD) from the structures calculated by mathematical formulas given according to crystal informatics in the PDB files. However, after optimization, all the HBs were revealed. The correct hybrid skill of optimization algorithms is also worth having a mention here. In the short comments, the author revisited two recently revealed Crystal structures of PrP segments with ‘polar collapse’ and found extra HBs in the network after optimization. The manuscript is clear written. Here we discuss more on comparing the structures in the PDB library and those after optimizations. How far away the current structures deposited in the PDB library from the refined structures are listed as follows. For 6AXZ.pdb, its RMSD [12] values are 0.077589, 0.058435, 0.075521, and 0.098501 angstroms for ABCD Chains, AB Chains, AC Chains, and ACE Chains respectively. For 6BTK.pdb, its RMSD values are 0.056441, 0.045499, and 0.075953 angstroms for AB Chains, AC Chains, and ACE Chains respectively. These RMSD values could further highlight the importance/necessity of refinement in the protein structure study.

In this paper, we revisited the ‘polar clasps’ in the structures of PrP and presented detailed HBs of the “polar clasps” after optimization. It is possible that different optimization strategies would have made different results. However, if the local searches in Swiss-PdbViewer 4.1.0 were carried out thoroughly, the optimization results should be the same ones.

## Acknowledgments

This research was supported by a Melbourne Bioinformatics grant numbered FED0001 on its Peak Computing Facility at the University of Melbourne, an initiative of the Victorian Government (Australia). The author thanks Rodriguez JA (University of California Los Angeles) for his helps to understand their paper [2] deeply. The author is also grateful to some comments from reviewers, which have improved this paper greatly.

## References

- [1] Sawaya MR, Sambashivan S, Nelson R, Ivanova MI, Sievers SA, Apostol MI, Thompson MJ, Balbirnie M, Wiltzius JJ, McFarlane HT, Madsen A, Riekel C, Eisenberg D (2007) Atomic structures of amyloid cross- $\beta$  spines reveal varied steric zippers. *Nature* 447(7143):453–457
- [2] Gallagher-Jones M, Glynn C, Boyer DR, Martynowycz MW, Hernandez E, Miao J, Zee CT, Novikova IV, Goldschmidt L, McFarlane HT, Helguera GF, Evans JE, Sawaya MR, Cascio D, Eisenberg DS, Gonen T, Rodriguez JA (2018) Sub-ngstrm cryo-EM structure of a prion protofibril reveals a polar clasp. *Nat Struct Mol Biol* 25(2):131–134
- [3] Zhang JP (2016) Mathematical formulas for prion all cross- $\beta$  structures listed in the Protein Data Bank. *Med Chem* 6(3):179–188
- [4] Yu L, Lee SJ, Yee VC (2015) Crystal structures of polymorphic prion protein  $\beta$ 1 peptides reveal variable steric zipper conformations. *Biochemistry* 54(23):3640–3648
- [5] Kozin SA, Bertho G, Mazur AK, Rabesona H, Girault JP, Haertl T, Takahashi M, Debey P, Hoa GH (2001) Sheep prion protein synthetic peptide spanning helix 1 and beta-strand 2 (residues 142-166) shows beta-hairpin structure in solution. *J Biol Chem* 276(49):46364–46370
- [6] Apostol MI, Perry K, Surewicz WK (2013) Crystal structure of a human prion protein fragment reveals a motif for oligomer formation. *J Am Chem Soc* 135(28):10202–10205
- [7] Humphrey W, Dalke A, Schulten K (1996) VMD: visual molecular dynamics. *J Mol Graph* 14(1):33–38

- [8] Guex N, Peitsch MC, Schwede T (2009) Automated comparative protein structure modeling with SWISS-MODEL and Swiss-PdbViewer: a historical perspective. *Electrophoresis* 30 Suppl 1:S162–173
- [9] Guex N, Peitsch MC (1997) SWISS-MODEL and the Swiss-PdbViewer: An environment for comparative protein modeling. *Electrophoresis* 18: 2714–2723
- [10] Zhang JP (2011) Derivative-free hybrid methods in global optimization and applications in December 2010. LAMBERT Academic Publishing, Germany. ISBN 978-3-8454-3580-0 (Available online <http://researchonline.federation.edu.au/vital/access/HandleResolver/1959.17/137122>)
- [11] Zhang JP (2015) *Molecular Structures and Structural Dynamics of Prion Proteins and Prions: Mechanism Underlying the Resistance to Prion Diseases*. Springer, Dordrecht. ISBN:978-94-017-7317-1
- [12] Zhang JP (2018) *Molecular Dynamics Analyses of Prion Protein Structures (1st ed. 2018 Edition): The Resistance to Prion Diseases Down Under*, Springer, Singapore. ISBN 978-981-10-8814-8